

Diaphragm Tracking in Cardiac C-Arm Projection Data

Marco Bögel¹, Andreas Maier², Hannes G. Hofmann¹, Joachim Hornegger¹,
Rebecca Fahrig³

¹Pattern Recognition Lab, Universität Erlangen-Nürnberg, Germany

²Siemens AG, Healthcare Sector, Forchheim, Germany

³Department of Radiology, Lucas MRS Center, Stanford University, Palo Alto, CA,
USA

`marco.boegel@informatik.stud.uni-erlangen.de`

Abstract. Long acquisition times of several seconds lead to image artifacts in cardiac C-arm CT. These artifacts are mostly caused by respiratory motion. In order to improve image quality, it is important to accurately estimate the breathing motion that occurred during image acquisition. It has been shown that diaphragm motion is correlated to the respiration-induced motion of the heart. We describe the development of a method that is able to accurately track the contour of the diaphragm in projection space. Therefore, the contour is modelled as a 2-D quadratic curve. In order to provide robust and stable tracking, additional constraints based on prior knowledge of the projection geometry and human anatomy are introduced. Results show that the tracking is very accurate. A mean model error per pixel of 0.93 ± 0.44 pixels was observed. The diaphragm top is tracked with an even lower error of only 0.62 ± 0.60 pixels.

1 Introduction

Cardiac C-arm CT makes it possible to reconstruct 3-D images during medical procedures. However, the long acquisition time of several seconds, during which the heart is beating and the patient might breathe, may lead to artifacts, such as blurring or streaks. A commonly used technique to reduce breathing motion is the single breath-hold scan. The physician instructs the patient to hold his breath after exhalation. The data is then acquired during the breath-hold. Although this approach is widely used, several studies have shown that breath-holding does not eliminate breathing motion entirely. Monitoring the position of the right hemidiaphragm during breath-hold, Jahnke et al. observed residual breathing motion to different extent for almost half their test group [1]. Therefore, it is necessary to develop better methods to estimate and compensate for respiratory motion in cardiac CT.

There are many ways to acquire respiratory signals. Most are based on additional equipment, e.g. Time of Flight- or Stereovision-cameras. Other techniques aim to extract the respiratory signal directly from the projection images. This

way the signal is perfectly in sync regarding the acquisition time of images and signal. Image-based respiratory motion extraction often relies on tracking of fiducial markers in the projection images [2,3]. Wang et al. have shown that the motion of the diaphragm is highly correlated to respiration-induced motion of the heart [4]. Sonke et al. propose to extract a one-dimensional breathing signal by projecting diaphragm-like features on the crano-caudal axis and selecting the features with the highest temporal change [5]. However, the downside to this approach is that the extracted signal is not the real respiration signal. Due to perspective projection, the projected amplitude is dependent on the C-arm rotation angle. In this work, we propose to track the diaphragm in a set of rotational projection images.

2 Materials and Methods

In this section we propose a method that aims to model the 2-D projection of a hemidiaphragm as a 2-D quadratic function. Most approaches for motion estimation based on tracking of features, assume that the features are unique objects, e.g. spherical fiducial markers. Unlike those methods, the object to be tracked here is not unique. The diaphragm appears as two similar parabolic shapes – the left and right hemidiaphragm.

2.1 Pre-Processing

The proposed method works automatically, with the exception of the manual selection of a start point in the first image. This user interaction is not required to be very accurate, the point has to be placed only in the rough perimeter of the top of one hemidiaphragm. Next, we define a Region of Interest (ROI) symmetrically around this point. A rectangular ROI is built in a way that it includes ideally only the contour of the selected hemidiaphragm. In Section 2.2 we explain how to estimate the diaphragm contour even with other structures present in the ROI. We propose an ROI of size 250×55 for projection images of size 640×480 . Figure 1 shows an inaccurately selected start point which is still working, and the ROI created around it. In order to reduce noise, the images are then smoothed with a gaussian kernel. After this, the Canny Edge Detector [6] is applied to extract the diaphragm contour. The hysteresis thresholding is done using percentiles of the edge magnitudes greater than zero. The low threshold was set to the 20th percentile, the high threshold to the 70th percentile.

2.2 Model Estimation

The result is a set of edge points that can now be used to estimate a quadratic model of the hemidiaphragm. However, due to the moderately chosen thresholds in the previous step, this set of points includes many false-positives which are not part of the diaphragm contour. To deal with this, the quadratic model is fit using the Random Sample Consensus (RANSAC) proposed by Fischler and

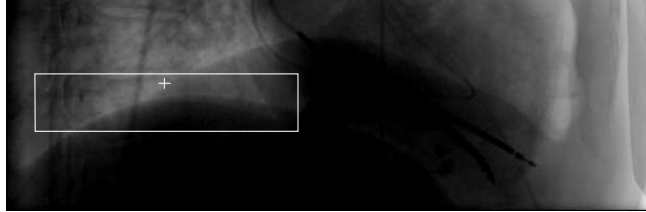


Fig. 1. User selected start point and initial rectangular ROI.

Bolles [7]. RANSAC can deal with datasets with large percentages of gross errors, and is thus the ideal choice to fit a model to our very noisy set of points. The diaphragm is of approximately parabolic shape, and is therefore estimated as a quadratic function $y = ax^2 + bx + c$. Thus, RANSAC has to estimate the three parameters a , b , and c . In the first step, three random points are selected. The model estimation can then be formulated as the following optimization problem

$$\sum_{i=1}^3 a \cdot x_i^2 + b \cdot x_i + c - y_i \rightarrow \min. \quad (1)$$

This way N (here: $N = 20000$) different models are fit to the data, which are then evaluated to determine the one that fits the data best. The model's quality is determined by the number of inliers. An inlier is a point that lies within a predefined distance to the model. Since an accurate model is desired we only consider points with a one pixel distance to the model inliers.

So far, the presented method has been very basic, it will find a contour, but it is not able to distinguish between the two different hemidiaphragms in case they are both visible in the ROI. Still, there are many additional constraints, based on prior knowledge, that can be enforced on the models. First of all, the diaphragm's opening is always facing down. Furthermore, assuming small motion between two subsequent frames, the curve's horizontal translation m_x can be limited by a multiple of the average translation \bar{m}_x . Also, the contour should only deform slowly over time, this can be enforced by limiting the change in the parabola's opening to $\frac{|a_{i-1} - a_i|}{a_{i-1}} < 0.05$, where a_i is the parameter a in the i -th image.

While the previous constraints already work most of the time, the algorithm still fails if the two hemidiaphragms are located close to one another and the models resembling their contours are similar. For this purpose, the prior knowledge of the patient's position and the C-arm rotation geometry can be utilized. Suppose acquisition starts from the right lateral view. Rotating towards the frontal view, the contour of the right hemidiaphragm will move to the left, whereas the contour of the left hemidiaphragm moves to the right. From the frontal position to the left lateral position this motion is reversed. We can now enforce the model to move in one direction until the turning point, and then move in the opposite direction. However, since the diaphragm is deforming during respiration, it

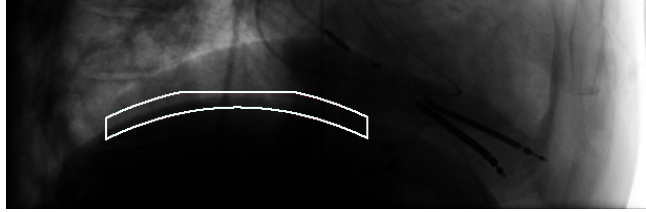


Fig. 2. Parabolic ROI used during tracking.

is better to loosen this constraint, by allowing free-motion around the turning point. So we finally have four constraints each valid model has to fulfill:

1. Diaphragm opening downwards: $a_i > 0$
2. Small motion assumption (deformation): $\frac{|a_{i-1}-a_i|}{a_{i-1}} < 0.05$
3. Small motion assumption (translation): $m_x < 3 \cdot \bar{m}_x$
4. Motion based on C-arm trajectory:
 - dir == dir_A , if start \leq angle $\leq 60^\circ$
 - dir == dir_B , if $120^\circ \leq$ angle \leq end

Models that do not fulfill all of the above can be discarded immediately. The constraints can be evaluated before the more costly determination of the number of inliers, thus even saving computation time.

2.3 Tracking

In order to track the contour throughout the entire image sequence, the ROI has to be moved. This is done by setting the seed point of the ROI to the vertex of the newly estimated model.

Finally, one last optimization can be made. After a model was computed for the first image, we know approximately how the contour has to look in the next image, due to the small motion assumption. The ROI can now be reshaped based on the last estimated model. The new parabolic ROI is then defined as the intersection of the rectangular ROI and the points $\mathbf{p} = (x, y \pm r)^T$, where x and y must satisfy the equation $y = a_{i-1}x^2 + b_{i-1}x + c_{i-1}$, with a_{i-1} , b_{i-1} , and c_{i-1} being the estimated model parameters of the previous image, and the variable r being the vertical radius of the parabolic ROI. The radius r is typically much smaller than the height of the rectangular ROI. Therefore, we are able to greatly reduce the number of considered false-positives, further improving the performance of the RANSAC algorithm. Figure 2 shows a parabolic ROI with radius $r = 10$.

3 Results

The accuracy of the proposed approach was evaluated on XCAT [8] projections of a breathing thorax. Our algorithm was used to track the left hemidiaphragm.

Width	Mean	Std. Dev.	Max
250	0.93	0.44	5
30	0.55	0.44	2
0	0.62	0.60	2

Table 1. Model error evaluated on windows with different widths around the vertex.

Projections of only the left hemidiaphragm were used as gold standard. The projection images were 640 pixels wide and 480 pixels high. A ROI of 250×55 pixels was used. All results are given in pixels.

First, we evaluate how well the model fits the reference contour. Therefore, the absolute difference of the model’s and the contour’s y -coordinates is computed. This error is computed over a specified window with the model’s vertex as its center and is then normalized by the width. Table 1 shows the normalized error evaluated at three different evaluation widths. The width of 250 evaluates the entire ROI that was used to estimate the model. For the range of zero only the error at the model’s vertex was computed. Additionally, the width of 30 presents a more balanced estimate for the error at the diaphragm top.

In order to further evaluate the accuracy of the model’s vertex in x and y direction, we computed the Euclidean distance between the vertex and the true maximum of the contour in the image. A mean Euclidean distance of 0.62 pixels and a standard deviation of 0.60 was observed.

Figure 3 shows the estimated model of the diaphragm in clinical projection data at four projection angles (0° corresponding to the lateral view).

4 Discussion

As results show, the proposed method allows us to track the diaphragm in projection data with very high accuracy. The model error is slightly higher when considering larger parts of the model. This is expected because of the diaphragm’s

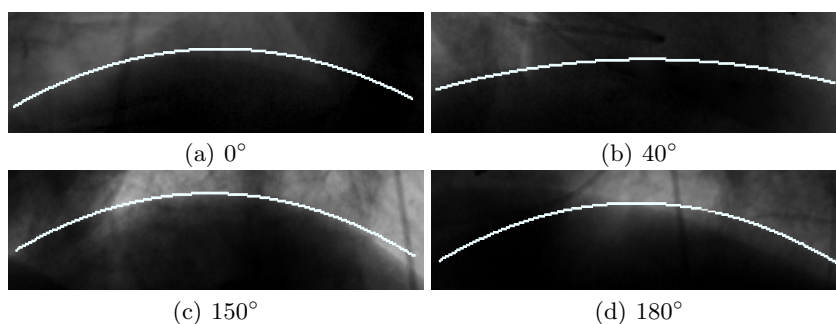


Fig. 3. Diaphragm tracking on clinical data.

asymmetry. A parabolic model is not a perfect fit for every perspective. Nevertheless, the diaphragm top can still be tracked very accurately, even if the real contour is asymmetric. This is sufficient for compensation of respiratory motion as previous studies have shown that it is highly correlated to the respiratory motion of the heart [4]. A very low Euclidean distance of 0.62 ± 0.60 proves that the vertex of the parabolic model is an excellent estimate of the diaphragm top. Visual inspection of tracking results in clinical projection data suggests equally good accuracy as the tracking in phantom data.

The presented method works well even if parts of the diaphragm are occluded due to bad contrast or overlap with other organs, e.g. the heart. However, high density objects, e.g. catheters, that are located close to the diaphragm contour have to be interpolated. Otherwise the parabola might be pulled towards them.

Future work will deal with the extraction of a 1-D respiratory signal based on the tracked position of the diaphragm top. The respiratory signal can then be used to compensate for respiratory motion in cardiac reconstruction.

References

1. Jahnke C, Paetsch I, Achenbach S, Schnackenburg B, Gebker R, Fleck E, et al. Coronary MR Imaging: Breath-hold Capability and Patterns, Coronary Artery Rest Periods, and beta-Blocker Use. *Radiology*. 2006;239:71–78.
2. Wiesner S, Yaniv Z. Respiratory Signal Generation for Retrospective Gating of Cone-Beam CT Images. In: *Proc. SPIE Med. Imaging*. vol. 6918 of *Proc. of the SPIE*. SPIE; 2008. p. 691817–1 – 691817–12.
3. Marchant TE, Price GJ, Matuszewski BJ, Moore CJ. Reduction of motion artefacts in on-board cone beam CT by warping of projection images. *Br J Radiol*. 2011 March;84:251–264.
4. Wang Y, Riederer S, Ehman R. Respiratory motion of the heart: Kinematics and the implications for spatial resolution in coronary imaging. *Magn Reson Med*. 1995;33:716–719.
5. Sonke JJ, Zijp L, Remeijer P, van Herk M. Respiratory correlated cone beam CT. *Med Phys*. 2005;32:1176–1186.
6. Canny FJ. A Computational Approach to Edge Detection. *IEEE Trans Pattern Anal Mach Intell*. 1986;8(6):679–698.
7. Fischler MA, Bolles RC. Random sample consensus: a paradigm for model fitting with applications to image analysis and automated cartography. *Communications of the ACM*. 1981 June;24:381–395.
8. Segars WP, Mahesh M, Beck TJ, Frey EC, Tsui BMW. Realistic CT Simulation Using the 4D XCAT Phantom. *Med Phys*. 2008;35(8):3800–3808.